Indian Journal of Pure & Applied Physics
Vol. 53, March 2015, pp. 181-189

Electronic and optical properties of $GaInX_2$ (X=As, P) from first principles study

Hamza Bennacer[a,c,*], Smail Berrah[b], Abdelkader Boukortt[c] & Mohamed Issam Ziane[a]

[a]Applied Materials Laboratory, Research Center, Sidi Bel Abbes University 22000, Algeria

[b](LMER) Laboratory, University A/ MIRA of Bejaia 06000, Algeria

[c]Elaboration and Characterization Physical Mechanics and Metallurgical of Material Laboratory, ECP3M, Electrical Engineering Department, Faculty of Sciences and Technology, Abdelhamid Ibn Badis University, Mostaganem 27000, Algeria

*E-mail: hamza_max28@yahoo.fr

Received 25 May 2014; revised 2 July 2014; accepted 28 December 2014

The structural, electronic and optical properties of $GaInAs_2$ and $GaInP_2$ with chalcopyrite structure in ternaries compounds have been studied in the present paper. To obtain accurate results, we have based our research on three phases. In the first phase, we used the first-principles calculations by using the full potential-linearized augmented plane wave method (FP-LAPW) within the density functional theory (DFT). In the second phase, the structural properties as exchange-correlation potential, the generalized gradient approximation (GGA-PBE Sol) of Perdew and al and local density approximation (LDA) of Perdew and Wang have been used. And in phase three, in order to get best values of the band gap, we used the developed form of GGA proposed by Engel–Vosko (EV-GGA) and the modified Becke-Johnson (mBJ) of Tran and Blaha, which are based on the optimization of total energy and corresponding potential. The compounds of $GaInP_2$ and $GaInAs_2$ demonstrate semiconducting behaviour with the direct-band gap of 0.3 and 2.03 eV using mBJ approach. The dielectric function, refractive index, reflectivity, absorption coefficient have been studied and the optical conductivity functions are calculated for radiation up to 20 eV. The obtained results indicate that $GaInP_2$ and $GaInAs_2$ are attractive materials for optoelectronic and photovoltaic applications.

Keywords: FP-LAPW, Chalcopyrite, Electronic band structure, Linear optical properties

1 Introduction

Light emission and photovoltaic effect may largely be the most important aspects of interest for a material to be used in optoelectronic applications[1]. Currently, in the field of light-emitting diodes, non-linear optic and photovoltaic sensitive material, chalcopyrite compounds have received much attention because of their potential properties[2].

Recently, the main abundant and reliable source of energy is the sun. This fact explains the attracting special attention about the photovoltaic solar energy converters. Yet the high cost and low efficiency of solar cells have restrained their wide use in daily life. Any materials that may be used in solar cells fabrication need possess a high absorption coefficient and a direct large enough gap suitably close to 1.4 eV to absorb light of the visible spectrum as well[1,3,4]. The commonly used materials for photovoltaic applications are amorphous, crystalline silicon and cadmium telluride (CdTe) in addition to chalcopyrites[1,5].

Gallium indium phosphide (GaInP) is a semiconductor composed of indium, gallium and phosphorus. It is used in high-power and high-frequency electronics because of its superior electron velocity with respect to more common semiconductors such as silicon and gallium arsenide[6].

The first $GaInP_2$ homojunction and $GaInP_2$/GaAs cascade solar cells have been produced and characterized. For both devices, the efficiencies are limited by a low short-circuit current density from the $GaInP_2$ homojunction. However, for the $GaInP_2$/GaAs cascade device, an open-circuit voltage of 2.17 V was achieved, one of the highest ever reported[7]. The principal application of GaInAs is as an infrared detector. GaInAs photodiodes are the preferred choice in the wavelength range 1.1-1.7 μm. For example compared to photodiodes made from Ge, GaInAs photodiodes were invented in 1977 by Pearsall[8], have faster time response, higher quantum efficiency and lower dark current for the same sensor area[9].

The $GaInP_2$ is a very important semiconductor compound in solar cells applications. The band gap of $GaInP_2$ can be varied as much as 100 meV in metal-organic chemical vapour deposition (MOCVD) grown

material by adjusting growth parameters that affect the degree of Cu-Pt ordering and chalcopyrite[10] (CH). These changes in the band gap of $GaInP_2$ due to ordering can be exploited in the design of III-V solar cell devices[10] and in combination with aluminium (AlGaInP alloy) to make high brightness LEDs with orange-red, orange, yellow and green colors[11].

Other important innovations include the integrated photodiode-FET receiver and the engineering of GaInAs focal-plane arrays[12].

In the present work, the structural, electronic and optical properties of the chalcopyrite ternaries $GaInAs_2$ and $GaInP_2$ semiconductors have been studied by using the full potential linearized augmented plane wave (FPLAPW) method[13] based on density functional theory[14-16] (DFT). Firstly, we have studied the chalcopyrite structure and described the theoretical procedure adopted to obtain the structural properties and total energies, where we have used a full total energy minimization for, firstly, obtaining the equilibrium *c/a* ratio and, secondly, we determined the equilibrium volume, bulk moduli and their derivative for this calculated *c/a* ratio. The electronic band structure, the density of states and the optical properties have also been studied in the present paper.

2 Computational Details

The present calculations are performed using the full-potential linearized augmented plane wave (FP-LAPW) method[17,18] as incorporated in Wien2k package[19].We take into account the III-III-V_2 ternary compounds in body-centered tetragonal chalcopyrite structure (space group I^-42d) with 8 atoms in the unit cell as shown in Fig. 1(a and b), the lattice constant *a* corresponding to the lattice constant of a cubic zinc blende structure, the *c/a* ratio, and the internal displacement parameter *u* revealing the distortion of the anion sublattice due to different surroundings. In the ideal structure[20], $c/a = 2$ and $u = 1/4$.

In order to achieve energy eigen values convergence, the wave functions in the interstitial regions were expanded in plane wave with a cut-off $R_{MT} \times K_{max} = 8$, where R_{MT} is the minimum radius of the muffin-tin spheres and K_{max} gives the magnitude of the largest *k* vector in the plane wave expansion. Inside the spheres, the valence wave functions were expanded up to $l_{max} = 10$. In order to keep the same degree of convergence for all the lattice constants, we kept the values of the sphere radii and K_{max} constant over all the range of lattice spacing considered. However, R_{MT} (R_{MT} are the smallest muffin-tin radius in the unit cell) was chosen for the expansion of the wave functions in the interstitial region while the charge density is Fourier expanded up to $G_{max} = 14$ $(Ryd)^{1/2}$.The R_{MT} chosen values in our calculations for Ga, In, P and As are, 2.1, 2.2, 2.0 and 2.1 a.u., respectively.

The exchange-correlation potential for structural properties was treated using the generalized gradient approximation (GGA PBEsol) of Perdew *et al*[21]. and the (LDA) of Perdew and Wang[22]. While for electronic and linear optical properties the Engel-Vosko-GGA (EV-GGA) formalism[23] is applied to optimize the corresponding potential for calculating the band structure[24]. Moreover, we did apply the modified Becke-Johnson[24-26] (mBJ) which is seen as a promising tool for accurate determination of the

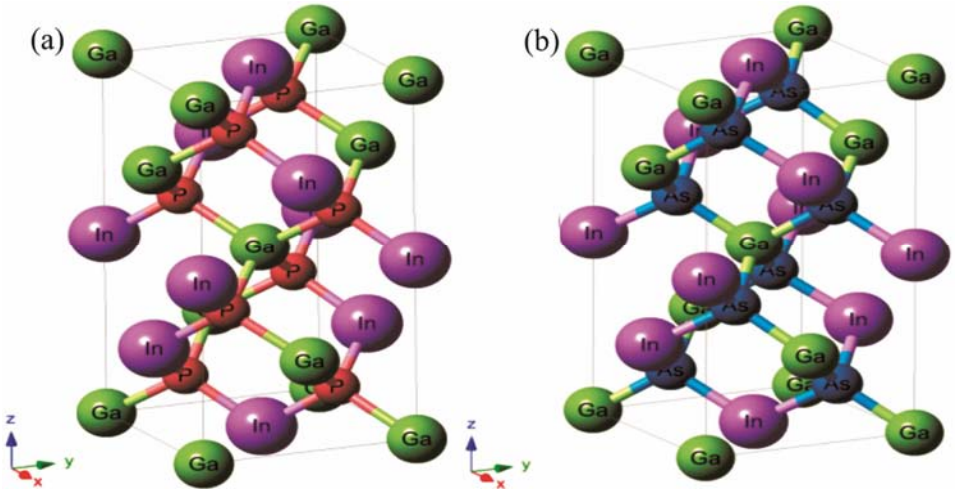

Fig. 1 — (a) Crystal structure of $GaInP_2$, (b): Crystal structure of $GaInAs_2$

fundamental band gaps of wide-band-gap materials[1,25-27].

The self-consistent calculations are considered to be converged when the total energy of the system is stable[28,29] within 10^{-4} Ryd. The integrals over the Brillouin zone (BZ) are performed up to 102 k-points, (grid of 10_10_10 meshes, and equivalent to 1000 k-points in the entire BZ).

In the optical properties calculations,we used the equivalent to 20000 k-points in the entire BZ by the OPTIC code[30] as implemented in the all-electron WIEN2K method[19]. It has been shown by Del Sole and Girlanda[31], GGA PBEsol, EV-GGA and mBJ are combined with the scissor-operator approximation to describe the optical spectrum rather accurately.

We have, therefore, made a correction ΔE_g to the gaps. The corrections to the FP-LAPW band gaps are ΔE_g = 0,369 eV for $GaInAs_2$ and ΔE_g = 0,026 eV for $GaInP_2$.

3 Results and Discussion

3.1 Geometry and Structure Optimization

The crystals of $GaInP_2$ and $GaInAs_2$ with chalcopyrite structure in ternary compounds are shown in Fig. 1(a and b), respectively. The optimized structural values are listed in Table 1.

We present the lattice constants (*a, c*) of chalcopyrite compound, the internal structural parameters *u,* the bulk modulus *B* and its first derivative *B′* of $GaInP_2$ and $GaInAs_2$, using LDA and GGA-PBE Sol approximations. It has been observed that the structure of this compound is rather similar to that of the ideal twice zinc-blende cell characterized by its rapport *c*/*a*=2 and its internal structural parameter *u*=0.25, which describe the position of (As/P) atoms.

To compare that fact, the available structural properties results in the study of Yeh *et al*[32]. and Seddiki *et al* [33]. have been considered to make it credible and validate our results. As it could be seen from Table 1, the computed lattice constants for $GaInAs_2$ and $GaInP_2$ are found to be in reasonable agreement with those obtained by Yeh *et al*[32]. using the tight binding calculations, and those calculated with FP-LAPW obtained by Seddiki *et al*[33].

In the case of the bulk modulus, our calculations predict the values of 54.09, 66.72 GPa for $GaInAs_2$ and 69.44, 81.007 GPa for $GaInP_2$ calculated using GGA PBE Sol and LDA. We may conclude, compared with the other data shown in Table 1, that the LDA and GGA lead to underestimating our calculated data. Our computed structural parameters are found to be in good agreement with the other previous data[32-34].

3.2 Electronics Properties

The electronic properties of $GaInAs_2$ and $GaInP_2$ in the chalcopyrite structure at the equilibrium lattice constant by using the GGA PBEsol, EV-GGA and mBJ approximations, have been calculated. The total densities of state for all approximation are shown in Figs 2 and 3. We have found a remarkable similarity behaviour between the results obtained with the three approximations used in our work. So, the results are discussed within mBJ only. It is clear that this approximation gives better values of the energy gap. The calculated band structure and total densities of state with mBJ approximation are shown in Fig. 4 for $GaInAs_2$ and in Fig. 6 for $GaInP_2$.

Table 2 presents the gap energy values for both compounds $GaInAs_2$ and $GaInP_2$ calculated with GGA-PBE Sol, EV-GGA and mBJ approximations, as compared with another calculation and

Table 1 — Calculated structural properties: lattice parameter *a, c,* bulk modulus *B* and its pressure derivative *B'* for the ternary compounds $GaInAs_2$ and $GaInP_2$ in the chalcopyrite structure

		a (Å)	c(Å)	c/a	*u*	B (GPa)	B′
	LDA	5.856	11.461	1.957	0.224	66.728	4.720
$GaInAs_2$	GGA	5.958	11.927	2.001	0.224	54.090	4.777
		5.866[a]	-	-	-	66.10[a]	-
	LDA	5.475	10.944	1.999	0.223	81.007	5.080
$GaInP_2$	GGA	5.660	11.300	1.996	0.269	69.443	4.576
		5.672[a]	-	-	-	80.070[a]	-
		5.740[b]	-	-	0.276[b]	67.537[b]	4.755[b]
		5.690[c]	-	-	-	77.050[c]	4.450[c]

[a]Tight binding calculations from Ref. (32).
[b]FP-LAPW calculations from Ref. (33).
[c]Theoretical data from Ref. (34).

experimental values. The mBJ calculation shows that $GaInAs_2$ and $GaInP_2$ are semiconductors with direct energy gap of 0.30 and 2.03 eV, respectively.

For further elucidation of the electronic band structure nature [35] the partial densities of state (PDOS) have also been calculated for those compounds within mBJ methods as shown in Fig. 5 for the $GaInAs_2$ and for the $GaInP_2$ in Fig. 7.

From Figs 4 and 5, we should emphasize that there are two distinct band structures in the density of electronic states in the $GaInAs_2$ in the valence band region. The lowest band is in the energy range between −11.8 and −9.6 eV originates from As_s states. The second region band is located between −6.3 eV and fermi energy (E_F) that is itself divided in two sub-bands, the first ranging from −6.3 and −3.8 eV which is, mainly, Ga_s and In_p states, while the second formed with significant contributions from As_p states. The conduction band ranging from 0.33 to 14.0 eV is principally composed of a mixture of Ga/In/As_ s,p states.

According to Figs 6 and 7, there are three distinct structures in the density of electronic states for the $GaInP_2$ separated by gap. The lowest structure in the energy range between −11.92 and −9.13 eV originates

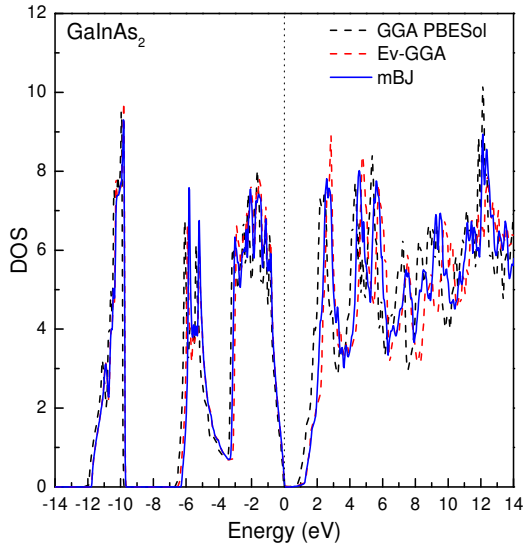

Fig. 2 — Calculated total density of state for $GaInAs_2$

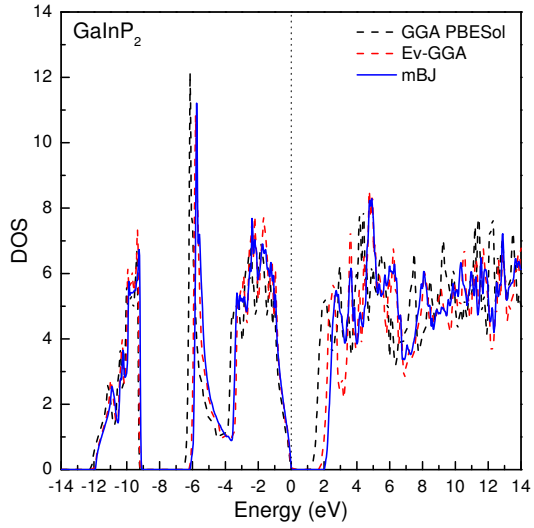

Fig. 3 — Calculated total density of state for $GaInP_2$

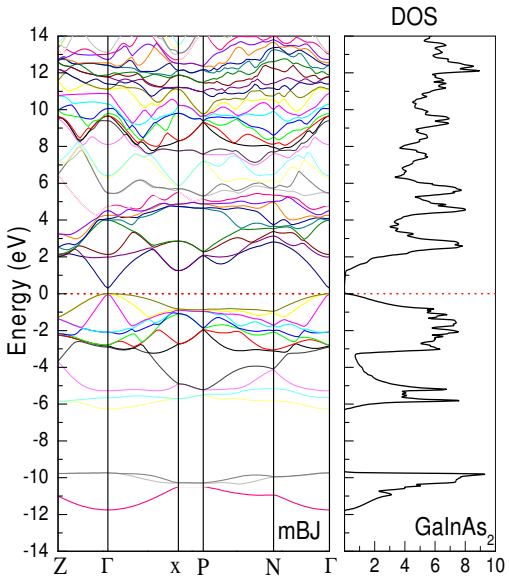

Fig. 4 — Calculated band structure and total density of state for $GaInAs_2$with mBJ approximation

Table 2 — Calculated energy gap of the two compounds $GaInAs_2$ and $GaInP_2$ with GGA-PBEsol, EV-GGA and mBJ approximations

Material	E_g (eV)				
	Our work GGAPBEsol	Our work EV-GGA	Our work mBJ	Other theoretical works	Exp.
$GaInAs_2$	0.000	0.224	0.304	0.917[a]	0.673-0.725[b]
$GaInP_2$	0.959	1.582	2.031	0.90[c] 1.44[d] 1.92[e] 2.013[f]	1.900[g] 2.005[h] 1.880[i]

[a]Ref. (36) ;[b]Ref (37); Experimental Data,[c]Ref. (33); PBE-GGA,[d]Ref. (33); EV-GGA.
[e]Ref. (33) mBJ-LDA,[f]Ref. (38) Pseudopotenial (LDA),[g]Ref. (39) ; Experimental Data.
[h]Ref. (40) ; Experimental Data,[I] Ref. (41) ; Experimental Data.

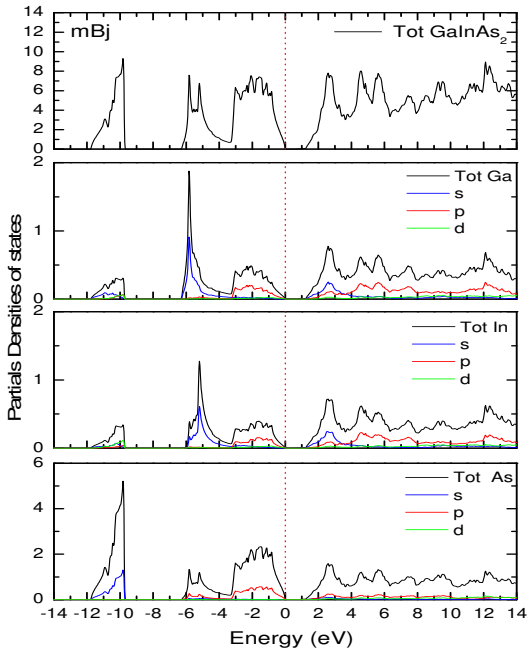

Fig. 5 — Partial densities of states of $GaInAs_2$with mBJ approximation

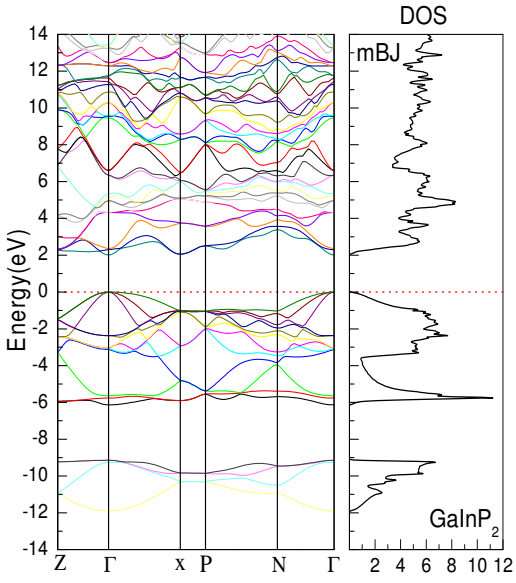

Fig. 6 — Calculated band structure and total density of state for $GaInP_2$ with mBJ approximation

from P_s states. The second region band is located between −6 eV and fermi energy (E_F) that is itself divided in two sub-bands, the first ranging from −6 to −3.6 eV which is, mainly, Ga/In_s states, while the second is formed of significant contributions from P_p states. The conduction band, the group ranging from 2.03 to 14.0 eV is mainly composed of Ga/In/P_ s, p states.

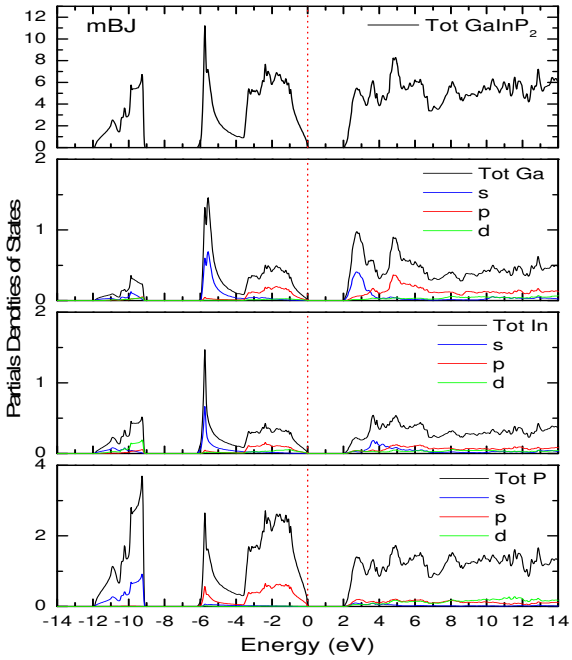

Fig. 7 — Partial densities of states of $GaInP_2$ with mBJ approximation

In Table 2, the fundamental band gaps (E_0) at the high-symmetry point Γ in the Brillouin zone have been listed for the investigated systems and the results have been compared with available experimental and theoretical data.

3.3 Optical Properties

The dielectric function, the refractive index, the absorption coefficient, and the optical conductivity of the ternaries chalcopyrite $GaInAs_2$ and $GaInP_2$ have been presented and calculated within mBJ approximation. As for scissor energy, the values of 0.369 eV and 0.026 eV for the $GaInAs_2$ and $GaInP_2$ consecutively have been used.

3.3.1 Dielectric Function

The optical properties are deduced from the dielectric function of the semiconductor given by the following equation[42]:

$$\varepsilon(\omega) = \varepsilon_1(\omega) + i\varepsilon_2(\omega) \qquad \ldots(1)$$

The values $\varepsilon_1(\omega)$ and $\varepsilon_2(\omega)$ are the real and imaginary parts, respectively at the same time. Based on the band-structure results, the dielectric function can be calculated. The dielectric function imaginary part $\varepsilon_2(\omega)$ is automatically obtained from the

electronic structure, once the joint density of states and the optical matrix overlap are used. The real part of the dielectric function $\varepsilon_1(\omega)$ is then calculated by the Kramers-Kronig relation. For calculating frequency dependent dielectric function $\varepsilon(\omega)$, we need energy eigenvalues and electron wave functions. The energy eigenvalues and electron wave function are the natural output for band structure calculation. Nevertheless, the imaginary part of the dielectric function depends on the joint density of state and the momentum matrix elements, while the real part is obtained from the Kramers-Kronig relation[42,43].The threshold energy occurs at E_0= 0.67 and E_0 =2.12 eV, which corresponds to the fundamental gap at equilibrium.

The imaginary dielectric function is a necessary quantity; it indicates the changing inter-band transitions in the semiconductor [42].The real and imaginary parts between 0 and 16 eV are shown in Figs 8 and 9 of $GaInAs_2$ and $GaInP_2$ already calculated within mBJ following two main crystallographic directions. Due to the tetragonal structure of the chalcopyrite crystals, the dielectric function is calculated for the two components $E\|c$ and $E\perp c$ of the dielectric function and all the parallel and perpendicular properties to the crystallographic axis c.

The real part shown in Fig. 8 is calculated by the Kramers–Kronig transformation. It has been seen that in the depressive part of the dielectric function $\varepsilon_1(\omega)$, the main features are fairly broad peaks around 2.52 and 3.09 eV for the two alloys $GaInAs_2$ and $GaInP_2$, respectively followed by a steep decrease between 4.24 and 4.73 eV for $GaInAs_2$ and between 4.37 and 5.06 for $GaInP_2$. After this energy range, $\varepsilon_1(\omega)$ becomes negative and takes a minimum value, then, slowly, increases towards zero at higher energies level. As shown in Fig. 8, the zero appears at 15.62 eV. The theoretical results are compared with experimental data, showing a good agreement.

Consequently, our calculated $\varepsilon_2(\omega)$ curve in Fig. 9 shows five sharp peaks at about 0.670, 0.912, 2.603, 4.612 and 5.977 eV for $GaInAs_2$. From its part, the calculated $\varepsilon_2(\omega)$ curve of $GaInP_2$ shows a sharp increase at about 2.028 eV at the first onset E_0 of the direct optical transitions. The first main peak is approximate to 2.116 eV, the second one draws near 3.164 eV. Concerning the third, the fourth and the fifth are located at 4.749, 5.071 and 6.055 eV, respectively.

In Fig. 10, we compared the calculated imaginary part of $GaInP_2$ within mBJ approximation with those calculated by Seddiki *et al*[33]. and the experimental data taken from Adachi *et al*[44].

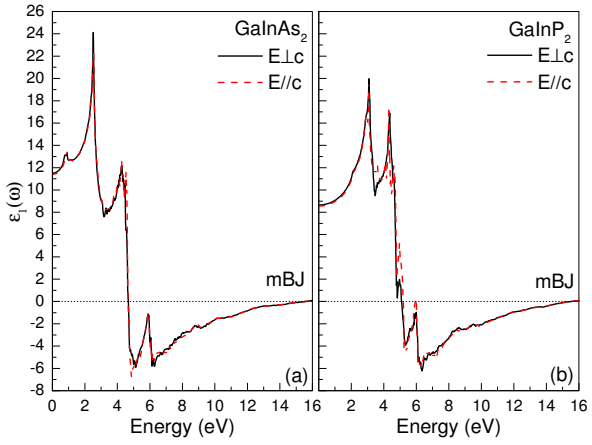

Fig. 8 — Real part of dielectric function: (a) $GaInAs_2$ and (b) $GaInP_2$

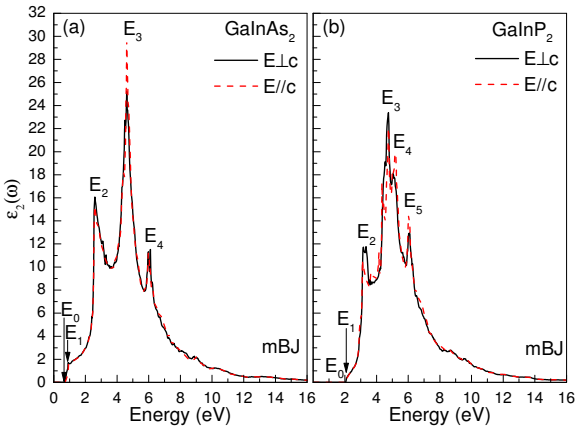

Fig. 9 — Imaginary part of dielectric function: (a) $GaInAs_2$ and (b) $GaInP_2$

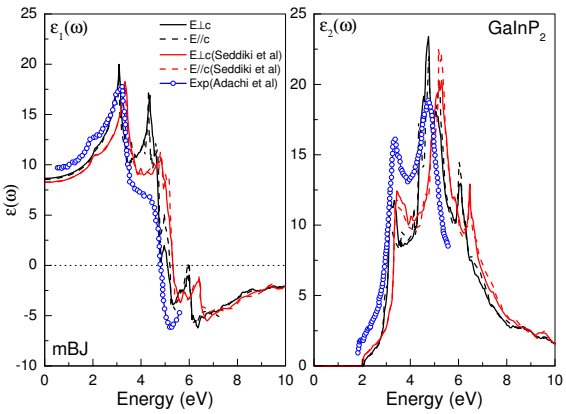

Fig. 10 — Real and Imaginary part of dielectric function for the $GaInP_2$ within mBJ

3.3.2 Refractive Index

The refractive index n is a very important physical parameter related to the microscopic atomic interactions.

$$n(\omega)=[\{(\varepsilon_1^2+\varepsilon_2^2)^{1/2}+\varepsilon_1\}^{1/2}/2^{1/2}] \quad \ldots(2)$$

Its values are often required to interpret various types of spectroscopic data. From theoretical view point, there are basically two different approaches in viewing this subject: on one hand, considering the crystal as a collection of electric charges. On the other hand, the refractive index will be related to the density and the local polarizability of these entities[42,45-47]. Any semiconductor refractive index $n(\omega)$ is computed through the real dielectric function[42]:

$$n=\sqrt{\varepsilon_1} \quad \ldots(3)$$

Figure 11 shows the refractive index of both compounds $GaInAs_2$ and $GaInP_2$ calculated with mBJ approach.The calculated static components of refractive index are presented in Table 3. The refractive index static values for low frequency related to the ternaries $GaInAs_2$ and $GaInP_2$ described by the relation $n(0)=\sqrt{\varepsilon_1}(0)$, $n(\omega)\perp$ having values 3.39, 3.94 and $n(\omega)\|$ having values 3.37, 2.91 do satisfy the relation $n(0)=\sqrt{\varepsilon_1}(0)$. The two polarizations non zero components of refractive index show maximum value at 4.97 and 4.51 eV for $GaInAs_2$ and $GaInP_2$ in order. The two components $n(\omega)\perp$ and $n(\omega)\|$ show weak isotropy at different range (0-10) eV.

3.3.3 Absorption Coefficient

The spectral components of absorption coefficient are shown in Fig. 12. The optical absorption coefficient $\alpha(\omega)$ is one of the most important evaluation criteria for the optoelectronic materials[47-50]. Our calculated absorption coefficient spectra $\alpha(\omega)$ for the herein investigated compounds as shown in Fig. 12, display that these materials have a good optical absorption in a wide energy range 0.7-10 eV and 2-10 eV for the $GaInAs_2$ and $GaInP_2$ in order of appearance. The deviation from the square-root dependence can be explained by the existence of a strong non-parabolic character of the contributing bands. It is obviously seen in the logarithmic representation used in Fig. 12. The absorption is determined by the expression:

$$\alpha(\omega)=(4\pi/\lambda)k(\omega) \quad \ldots(4)$$

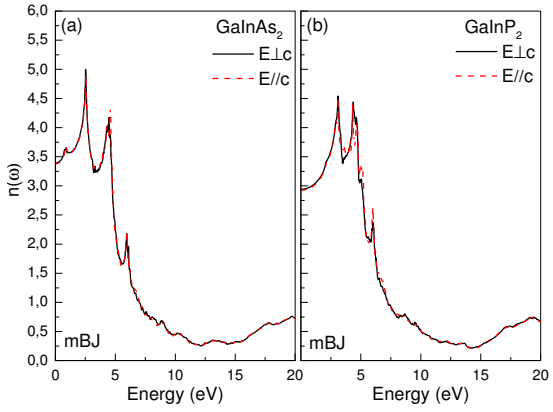

Fig. 11 — Calculated refractive index: (a) $GaInAs_2$ and (b) $GaInP_2$

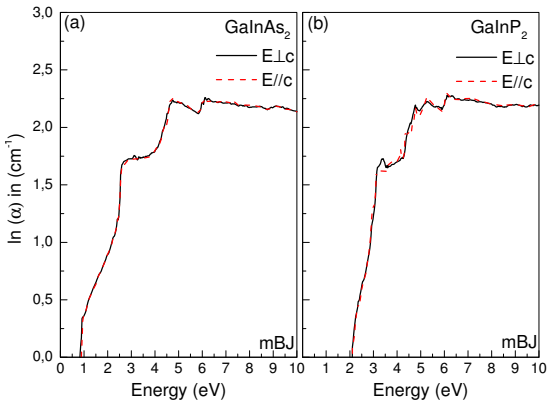

Fig. 12 — Absorption coefficient: (a) $GaInAs_2$ and (b) $GaInP_2$

Table 3 — Calculations peaks ($E\perp c$) in the imaginary dielectric function $\varepsilon_2(\omega)$, static optical parameters $\varepsilon_1(\omega)$ and $n(\omega)$ compared with other calculations and experimental values

	E_0	E_1	E_2	E_3	E_4	E_5	$\varepsilon_1(0)$	n(0)
$GaInAs_2$	0.670[a]	0.912[a]	2.603[a]	4.612[a]	5.977[a]	-	11.507[a]	3.391[a]
$GaInP_2$	2.028[a]	2.116[a]	3.164[a]	4.749[a]	5.071[a]	6.055[a]	8.652[a]	2.941[a]
	1.92[b]	2.098[b]	3.438[b]	5.215[b]	-	6.466[b]	8.259[b]	-
	-	1.926[c]	3.361[c]	4.726[c]	-	-	9.694[c]	-

[a]Present work,[b]Other calculation from Ref. (33),[c] Experimental data from Ref. (44).

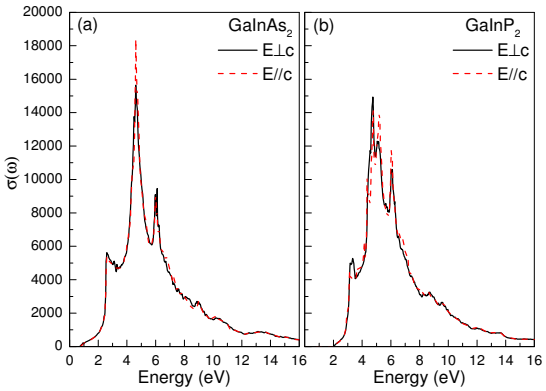

Fig. 13 — Optical conductivity: (a) $GaInAs_2$ and (b) $GaInP_2$.

Table 4 — Different peaks and their width of the optical conductivity for $GaInP_2$ and $GaInAs_2$ calculated within mBJ

Compounds	$GaInP_2$	$GaInAs_2$
Peak	4.599 eV	4.738 eV
Width	11.193eV	9.591eV

From the features of the absorption coefficient, the presence of three peaks has been noted. The first transition correspond to Gamma (Γ) point Γ_{15v}-Γ_{15c} and that second at 2.82 eV in $GaInAs_2$ and 3.39 eV in $GaInP_2$ representing a transition X_{15v}-X_{1c}. As for the last peak value, it is 4.76 eV, 5.20 eV corresponding to the transition L_{15v}-L_{1c} for the $GaInAs_2$ and $GaInP_2$, respectively.

The maximum value of the absorption coefficient shifts from 2.92 eV in $GaInAs_2$ to 3.37 eV in $GaInP_2$, while the second interesting feature is the appearance of the second peak around 4.74 eV in $GaInAs_2$ to 5.23 eV in $GaInP_2$. These two peaks explain maximum light absorption at two different wavelengths. Due to this material property, it can be used for wavelength filtering purposes in those regions.

There is a high absorption between 1ev and 10 eV for the $GaInAs_2$ alloy and between 2 eV to 10 eV for $GaInP_2$, related to wave lengths 1.24-0.124 μm and 0.62-0.124 μm for each.

3.3.4 Optical Conductivity

The optical conductivity is concluded from the dielectric function**.** It is given[42] by:

$$\sigma(\omega) = -(i\omega / 4\pi)\varepsilon(\omega) \qquad \ldots(5)$$

The curves of the optical conductivity versus energy calculated within mBJ approximation are shown in Fig. 13 for both ternaries $GaInP_2$ and $GaInAs_2$. The optical conductivity spectra using the imaginary part of the dielectric function have been studied. A range of energies between 0 and 16 eV hasbeen calculated. The curves present several peaks corresponding to the bulk plasmon excitations which are caused by electrons crossing from the valence to the conduction band. The positions of the main peak and the total widths of the optical conductivity for the different ternary compounds are compared in Table 4.

4 Conclusions

The research study presents new results concerning electronics and optical properties of the ternary compounds by using the FP-LAPW method within the modified Becke-Johnson exchange potential and other approximations. Moreover, the present calculation gives a direct band gap for our ternary compounds $GaInP_2$ and $GaInAs_2$.The study of the optical properties is important when the real and imaginary parts of the dielectric function have been determined as well as the assignment of the optical transitions under two types has been presented, which correspond to both polarizations ($E\perp c$ and $E\|c$). We have shown that it is possible to improve band gap calculations by combining GGA-PBEsol, EV-GGA and mBJ. With such modification, a good result with mBJ approximation has been obtained.

Our predicted band gaps dependent on optical parameters such as the refraction index, dielectric constant, and optical conductivity are calculated and analyzed in this paper. The prominent variations in the optical parameters make $GaInP_2$ suitable for optical devices in the major parts of the spectrum. These ternaries present a particular interest in the area of optoelectronic devices and solar cell applications**.**

Acknowledgement

We are grateful to Dr. Tarik Ouahrani (Laboratoire de Physique Théorique, Université de Telmcen, Algeria), Dr. Miloud Ibrir (M'sila University, Algeria), Mr. Mohamed Azouze (Sidi Bel Abbes University, Algeria) and Mr. Benaissa Sid Ali (M'sila University, Algeria) for their valuable and useful discussions, help and orientations.

References

1 Shaposhnikov V L, Krivosheeva A V & Borisenko V E, *Phys Rev B*, 85 (2012) 205201.
2 T Ouahrani, Otero-de-la-Roza A & Khenata R, *Computational Materials Sci*, 47 (2010) 655.
3 Luque A, *J Appl Phys*, 110 (2011) 00031301.

4 Bube R H, *Photovoltaic Materials*, Imperial College Press, (1998) 1-33.
5 Rosencher E & Vinter B, *Optoelectronics*, Cambridge University Press, UK, (2002).
6 Plamer D W, *Semiconductors*, Co UK, (2006).
7 *Olson J M, Gessert T & Al-Jassim M M*, *Photovoltaic Specialists Conference*, New York, Institute of Electrical and Electronics Engineers, (1985) 552.
8 Wei S-H, L Ferreira G & Zunger A, *Physical Review B*, 41 (1990) 8240.
9 Wei S-H, Ferreira L G, Bernard J E & Zunger A, *Physical Review B*, 42 (1990) 9622.
10 Levi Dean H, Geisz John F & Johs Blaine, Proc *SPIE* 5530, Fourth International Conference on Solid State Lighting, 326 (2004) doi:10.1117/12.559973.
11 Vyas P S, Gajjar P N, Thakore B Y & Jani A R, *Physica B*, 406 (2011) 4412.
12 Leheny R F, Nahory R E & Pollack M A, *Electron* Lett, 16 (1980) 353.
13 Jansen H J F & Freeman A J, *Phys Rev B*, 30 (1984) 561.
14 Hohenberg P & Kohn W, *Phys Rev B*, 864 (1964) 136.
15 Sham L J & Kohn W, *Phys Rev*, 145 (1965) 561.
16 Perdew J P & Wang Y, *Phys Rev B*, 45 (1992) 13244.
17 Madsen G K H, Blaha P & Schwarzet K, *Phys Rev B*, 64 (2001) 64.
18 Schwarz K, Blaha P & Madsen G K H, *Compute Phys Commun*, 147 (2002) 147.
19 P Blaha, K Schwarz & G K H Madsen et al, WIEN2k,An Augmented Plane Wave Plus Local Orbital's Program for Calculating Crystal Properties (Vienna University of Technology, Vienna, Austria, ISBN 3-9501031-1-2, (2001).
20 Limpijumnong Sukit, Lambrecht Walter R L & Segall Benjamin, *Physical Review B*, 60 (1999) 8087.
21 Perdew J P, Ruzsinszky A & Csonka G I, *Phys Rev Lett*, 100 (2008) 136406.
22 Perdew J P & Wang Y, *Phys Rev* B, 45 (1992) 13244.
23 Engel E & Vosko S H, *Phys Rev B*, 47 (1993) 13164.
24 Ouahrani Tarik, Reshak H & Khenata, *Phys Status Solidi B*, 1–7 (2010) / DOI 10.1002/pssb.200945463.
25 Tran F & Blaha P, *Phys Rev Lett*, 102 (2009) 226401.
26 Koller D, Tran F & Blaha P, *Phys Rev B*, 83 (2011) 195134.
27 Becke A D & Johnson E R, *J Chem Phys*, 124 (2006) 221101.
28 Blochl P E, Jepsen O & Anderson O K, *Phys Rev B*, 49 (1994) 16223.
29 Annane F, Meradji H, Ghemid S & Hassan F El Haj, *Computational Materials Sci*, 50 (2010) 274.
30 Ambrosch-Draxl C & Sofo J O, *Compute Phys Communi*, 175 (2006) 1.
31 Sole R Del & Girlanda R, *Phys Rev B*, 48 (1993) 11789.
32 Yeh C-Y, Chen A B & Sher A, *Phys Rev B*, 43 (1991) 9138.
33 Seddiki N, Ouahrani Tarik & Lasriet B, *Materials Sci in Semicon Proc*, 16 (2013) 1454.
34 Lour W-S, Chang W-L & W-C Liu, *Appl Phys Lett*, 74 (1999) 2155.
35 Bin Xu, Xingfu Li & Zhen Qin, *Physica B*, 406 (2011) 946.
36 Teng D, Shen J, Newman K E & Gu B L, *J Phys Chem Solide*, 52 (1991) 1109.
37 Arent D J, *SPIE*, *Epitaxial Growth Proc*, 2141 (1994) 0-8194-1435-2/94.
38 Lee K-H, Lee S-G & Chang K J, *Physical Review B*, 52 (1995) 15862.
39 Deelen J Van, Bauhuis G J & Schermer J J, *J of Cryst Growth*, 298 (2007) 772.
40 Schubert M & Rheinlander B, *Physical Review B*, 54 (1996) 0163
41 Kozhevnikov M, Narayanamurti V & Mascarenhas A, *Appl Phys Lett*, 75 (1999) 1128
42 Berrah S, Boukortt A & Abid H, *Physica E*, 41 (2009) 701.
43 Fox M, *Optic Properti of Solids*, Oxford University Press, New York, (2001) 6.
44 Adachi S, Optical Constants of Crystalline and Amorphous Semi-conductors:Numerical Data and Graphical Information, KluwerAcademic, Boston, (1999).
45 Goldhahn R, Scheiner J & Shokhovets S, *Phys Status Solidi*, 216 (1999) 265.
46 Balzaretti N M & Jornada J A H da, *Solid State Comm*, 99 (1996) 943.
47 Boukortt A, S Berrah, R Hayn & A Zaoui, *Physica B*, 405 (2010) 763.
48 Bouhemadou A, Al-Essa S & Allali D, *Solid State Sci*, 20 (2013) 127.
49 Jani Omkar, Honsberg Christiana & Asghar Ali, the 31st*IEEE* Photovoltaic Specialists Conference, January, 3 (2005).
50 Amin B, Khenata R & Bouhemadouet A, *Physica B*, 407 (2012) 2588.